Terahertz time domain magneto-optical ellipsometry in reflection geometry

Y. Ino,[1] R. Shimano,[1,*] Y. Svirko,[2] and M. Kuwata-Gonokami[1,†]
[1]*Department of Applied Physics, The University of Tokyo and SORST, Japan Science and Technology Agency (JST), 7-3-1 Hongo, Bunkyo-ku, Tokyo 113-8656, Japan*
[2]*Department of Physics, University of Joensuu, P.O. Box 111, Fin-08101 Joensuu, Finland*
(Received 28 October 2003; revised manuscript received 21 July 2004; published 6 October 2004)

We propose and examine a method to reveal the diagonal and off-diagonal components of a dielectric tensor from THz magneto-optical Kerr effect (MOKE) measurements. The proposed method, which is based on time-domain THz measurement, does not involve any assumption on the magnitude of the magneto-optical constant. We apply this method to determine the dielectric tensor of *n*-type InAs in the spectral range from 0.5 to 2.5 THz and compare the results with those obtained in the framework of the conventional small magneto-optical response approximation. (SMRA). It is shown that when the probe frequency is lower than the frequency of longitudinal electromagnetic modes in the medium (e.g., below magnetoplasma or longitudinal phonon resonance) the SMRA-based analysis should be replaced with the method we developed even for small magneto-optical signals.

DOI: 10.1103/PhysRevB.70.155101 PACS number(s): 78.90.+t, 78.47.+p, 42.25.Ja

I. INTRODUCTION

The incorporation of the spin degree of freedom into semiconductor technology has resulted in the formation of a new discipline, spintronics, which deals with injection, transport, control and detection of spin-polarized charge carriers.[1] The development and implementation of spintronic devices will require detailed information on the kinetic, relaxation, and transport properties of spin subsystems that cannot be obtained by conventional magnetization measurements. The combination of magneto-optical measurements and advanced optical probing techniques enables us to probe such magnetic properties. With recent advances in ultrafast laser technology, both the temporal and spatial evolutions of the spin orientation and the coherence can be probed by using time-resolved magneto-optical measurements. For example, this technique has been employed to extract surface magnetization[2] and to probe ultrafast dynamics of bulk magnetization[3,4] in magnetic materials.

Magneto-optical Kerr effect (MOKE) measurements in a reflection configuration enable us to investigate materials that are opaque in the frequency region of interest[5–9] by analyzing the polarization azimuth rotation ϕ and ellipticity angle η of the reflected light wave. Usually, MOKE data are analyzed using the small magneto-optical response approximation (SMRA). In the SMRA framework, one assumes that (i) the off-diagonal component of the dielectric tensor, $\tilde{\epsilon}_{xy}$, is small compared to the diagonal component, $\tilde{\epsilon}_{xx}$ (i.e., $|Q| \ll 1$, where $Q=i\tilde{\epsilon}_{xy}/\tilde{\epsilon}_{xx}$ is the magneto-optical constant), and (ii) the change of the diagonal component induced by the magnetic field is negligible. Since in this approximation ϕ and η are proportional to $\tilde{\epsilon}_{xy}$, one can obtain the real and imaginary part of $\tilde{\epsilon}_{xy}$ directly from ϕ and η using complex refractive index measured with no magnetic field. If the medium has a large magneto-optical response, we need additional measurements to determine the components of the dielectric tensor. This can be done, for example, using the general ellipsometry technique that involves measurements of three polarization-dependent reflection coefficients.[10–13] However, in the THz frequency region we have even more opportunities. Specifically, THz measurements are performed in the time domain, so that information on the temporal evolution of the electric field on the THz wave is obtained. This information allows us to obtain both the amplitude and phase of the THz wave,[14,15] and can be used to obtain the diagonal and off-diagonal components of the dielectric tensor from experimental data acquired with a conventional MOKE scheme without using SMRA.

In this paper, we develop a method for evaluating the diagonal and off-diagonal components of the complex dielectric tensor in the THz frequency range from MOKE measurements. The method does not rely on any assumptions about the magnitude of Q and can be employed for materials with a pronounced magneto-optical response. In the developed method, by measuring the amplitude and phase of the reflected THz wave simultaneously, we obtained the real and imaginary parts of complex reflection coefficients, which allows us to calculate the real and imaginary parts of the diagonal and off-diagonal components of the dielectric tensor. This method is referred to as the time-domain THz ellipsomery. By using the results of our THz MOKE measurements in *n*-type InAs which revealed a large MOKE signal beyond the range of applicability of SMRA at oblique incidence,[16] we demonstrate that the developed method allows us to determine the complex dielectric tensor of the media with strong magneto-optical response. We also discuss the validity of the SMRA in the interpretation of the MOKE data by comparing SMRA predictions with results with the method we developed.

II. THEORY

In this section, we introduce a method that enables us to determine real and imaginary parts of $\tilde{\epsilon}_{xx}$ and $\tilde{\epsilon}_{xy}$ from complex reflection coefficients, which are obtained in MOKE measurements.

 ©2004 The American Physical Society

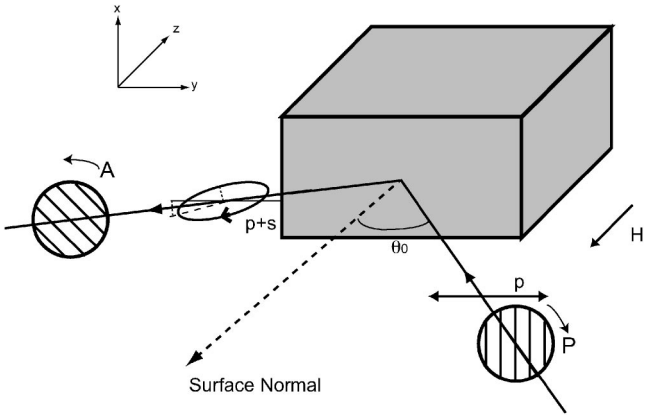

FIG. 1. Schematic illustration of the polar Kerr geometry. The magnetic field is antiparallel to the *z* axis of the laboratory Cartesian frame. The angles between optical axes of the polarizer and analyzer and *x* axis are labeled as *P* and *A*, respectively.

A. The MOKE signal at oblique incidence

The geometry of the experiment is shown in Fig. 1. In this geometry, the *p*-polarized wave is incident to the sample surface at the incidence angle θ_0, while the external magnetic field is applied along the surface normal. The polarization of the incident and reflected waves are controlled by the polarizer and analyzer, respectively. One can recall from Fig. 1 that such a geometry of the magneto-optical experiment is often referred to as the polar Kerr geometry. Correspondingly, in this paper, we will refer to the measured spectrum as the "magneto-optical Kerr effect spectrum." However, it is necessary to note that since the incidence angle is finite, the Voigt or Cotton-Mouton effect also contributes to the measured signal.

Since the fourfold symmetry axis is oriented along the surface normal (*z* axis of the Cartesian coordinate frame), the complex dielectric tensor can be presented in the following form:

$$\epsilon = \begin{pmatrix} \tilde{\epsilon}_{xx} & \tilde{\epsilon}_{xy} & 0 \\ -\tilde{\epsilon}_{xy} & \tilde{\epsilon}_{xx} & 0 \\ 0 & 0 & \tilde{\epsilon}_{zz} \end{pmatrix}. \tag{1}$$

To determine the components of the dielectric tensor, we need to relate them to the measurable complex reflection coefficients $\tilde{r}_{pp}$ and $\tilde{r}_{sp}$, where subscripts label polarization components of the reflected and incident wave. The lengthy but straightforward calculations shown in the Appendix allow us to obtain $\tilde{r}_{pp}$ and $\tilde{r}_{sp}$ as functions [detailed in Eqs. (A13) and (A14)] of $\tilde{\epsilon}_{xx}$, $\tilde{\epsilon}_{xy}$, and $\tilde{\epsilon}_{zz}$:

$$\tilde{r}_{pp} = \tilde{r}_{pp}(\tilde{\epsilon}_{xx}, \tilde{\epsilon}_{xy}; \tilde{\epsilon}_{zz}),$$

$$\tilde{r}_{sp} = \tilde{r}_{sp}(\tilde{\epsilon}_{xx}, \tilde{\epsilon}_{xy}; \tilde{\epsilon}_{zz}). \tag{2}$$

Since $\tilde{r}_{pp}$ and $\tilde{r}_{sp}$ are functions of three complex variables, we can calculate $\tilde{\epsilon}_{xx}$ and $\tilde{\epsilon}_{xy}$ from the obtained complex reflection coefficients as long as $\tilde{\epsilon}_{zz}$ is known.

By using conventional formulas for the polarization azimuth and ellipticity angle in terms of the Cartesian components of the electric field $\vec{E}$,[17]

$$\phi = \frac{1}{2}\tan^{-1}\frac{2\,\mathrm{Re}\,\tilde{E}_x\tilde{E}_y^*}{|\tilde{E}_x|^2 - |\tilde{E}_y|^2},$$

$$\eta = \frac{1}{2}\sin^{-1}\frac{2\,\mathrm{Im}\,\tilde{E}_x\tilde{E}_y^*}{|\tilde{E}_x|^2 + |\tilde{E}_y|^2}, \tag{3}$$

one can readily obtain ϕ and η in terms of $\tilde{r}_{pp}$ and $\tilde{r}_{sp}$:

$$\phi = -\frac{1}{2}\arg\left(\frac{\tilde{r}_{pp} - i\tilde{r}_{sp}}{\tilde{r}_{pp} + i\tilde{r}_{sp}}\right),$$

$$\eta = \tan^{-1}\left(\frac{|\tilde{r}_{pp} - i\tilde{r}_{sp}| - |\tilde{r}_{pp} + i\tilde{r}_{sp}|}{|\tilde{r}_{pp} - i\tilde{r}_{sp}| + |\tilde{r}_{pp} + i\tilde{r}_{sp}|}\right). \tag{4}$$

In Sec. II C, we will outline the procedure based on Eqs. (2) and (4) for evaluation of $\tilde{\epsilon}_{xx}$ and $\tilde{\epsilon}_{xy}$ from ellipsometric experiments.

B. Analysis based on the intensity measurement

Before considering in detail the time-domain THz ellipsometry, we revisit here a conventional MOKE technique at optical frequencies based on the light intensity measurements. In the MOKE intensity-based measurement technique, the polarization azimuth angle ϕ and ellipticity angle η of the reflected electromagnetic wave under the magnetic field are obtained.[18] Since ϕ and η depend only on the ratio $\tilde{r}_{sp}/\tilde{r}_{pp}$ [see Eq. (4)], both the real and imaginary parts of $\tilde{r}_{sp}/\tilde{r}_{pp}$ can be determined from the MOKE experiment.

When the SMRA conditions are fulfilled (i.e., when the magneto-optical response is small, $|Q| \ll 1$ and dependence of $\tilde{\epsilon}_{xx}$ on magnetic field is negligible), ϕ and η do not exceed a few degrees. In such a case Eqs. (2) and (4) are reduced down to the following SMRA equation:[9]

$$\begin{pmatrix} \phi \\ \eta \end{pmatrix} = \begin{pmatrix} \mathrm{Re} \\ \mathrm{Im} \end{pmatrix} \frac{n_0\tilde{\epsilon}_{xy}}{(\tilde{\epsilon}_{xx} - n_0^2)\sqrt{\tilde{\epsilon}_{xx}}} \frac{\cos\theta_0}{\cos(\theta_0 + \tilde{\theta})}, \tag{5}$$

where n_0 is the index of refraction of the air, and $\tilde{\theta}$ is the (complex) refraction angle that is defined by Snell's law. In Eq. (5) variables $\tilde{\epsilon}_{xx}$ and $\tilde{\epsilon}_{xy}$ are separated; therefore if we measure $\tilde{\epsilon}_{xx}$ independently (say, from the reflectivity at zero magnetic field), we can directly determine the real and imaginary part of $\tilde{\epsilon}_{xy}$ from the measured ϕ and η.

If the magneto-optical response is not small, SMRA is not applicable. In such a case the diagonal component of the dielectric tensor may not be negligible and we need to perform additional measurements to determine $\tilde{\epsilon}_{xx}$ and $\tilde{\epsilon}_{xy}$ even in the case of normal incidence. In particular, this can be done using the general ellipsometry technique.[10–13] In this technique, one measures $\tilde{R}_{pp} = \tilde{r}_{pp}/\tilde{r}_{ss}$, $\tilde{R}_{sp} = \tilde{r}_{sp}/\tilde{r}_{ss}$, and $\tilde{R}_{ps} = \tilde{r}_{ps}/\tilde{r}_{ss}$ by rotating the analyzer with a finite angular frequency,[11] while $\tilde{\epsilon}_{xx}$, $\tilde{\epsilon}_{xy}$, and $\tilde{\epsilon}_{zz}$ are obtained by fitting the measured reflection coefficients[13] using exact equations.[12]

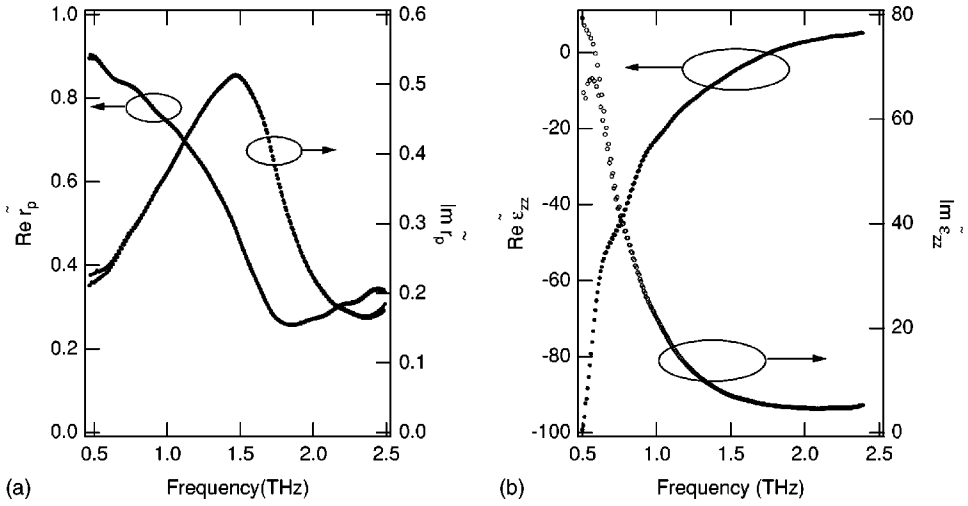

FIG. 2. The spectra of (a) $\tilde{r}_p$ and (b) $\tilde{\epsilon}_{zz}$. $\tilde{\epsilon}_{zz}$ is calculated from measured value of $\tilde{r}_p$.

C. Analysis based on the time-domain THz ellipsometry

In this paper we propose a method to determine $\tilde{\epsilon}_{xx}$ and $\tilde{\epsilon}_{xy}$ from experimentally obtained $\tilde{r}_{pp}$ and $\tilde{r}_{sp}$ providing that $\tilde{\epsilon}_{zz}$ was obtained from independent measurements. The method is based on time-domain THz spectroscopy technique and referred to as the time-domain THz ellipsometry. The THz spectroscopy technique enables us to reveal the temporal evolution of the THz electric field[14,15] and to obtain the phase and amplitude of the reflected THz wave, and the complex reflection coefficient. The technique reported in Ref. 16 gives both the real and imaginary parts of $\tilde{r}_{pp}/\tilde{r}_p$ and $\tilde{r}_{sp}/\tilde{r}_p$, where $\tilde{r}_p$ is a reflection coefficient which is determined from given $\tilde{\epsilon}_{zz}$. This procedure allows us to arrive at real and imaginary parts of $\tilde{r}_{pp}$ and $\tilde{r}_{sp}$, therefore, to obtain ϕ and η [see Eqs. (4)]. The next step includes rewriting Eq. (2) to obtain $\tilde{\epsilon}_{xx}$ and $\tilde{\epsilon}_{xy}$ in terms of $\tilde{r}_{pp}$ and $\tilde{r}_{sp}$ as follows:

$$\tilde{\epsilon}_{xx} = \tilde{\epsilon}_{xx}(\tilde{r}_{pp}, \tilde{r}_{sp}; \tilde{\epsilon}_{zz}),$$

$$\tilde{\epsilon}_{xy} = \tilde{\epsilon}_{xy}(\tilde{r}_{pp}, \tilde{r}_{sp}; \tilde{\epsilon}_{zz}). \tag{6}$$

Finally we can calculate $\tilde{\epsilon}_{xx}$ and $\tilde{\epsilon}_{xy}$ directly from the measured $\tilde{r}_{pp}$, $\tilde{r}_{sp}$, and given $\tilde{\epsilon}_{zz}$. One can notice that the phase information provided by the time-domain THz spectroscopy technique allows us to determine $\tilde{\epsilon}_{xx}$ and $\tilde{\epsilon}_{xy}$ from the measurable complex reflection coefficients without any restriction of the magnitude of the magneto-optical constant Q.

III. EXAMPLE OF THE ANALYSIS

In this section, we demonstrate how the developed procedure can be employed to obtain the complex dielectric tensor using the results of the THz MOKE measurements in an *n*-type InAs. The first step is to measure the complex reflectivity coefficient $\tilde{r}_p$ in the absence of the magnetic field. Since the crystal symmetry does not permit any current parallel to the magnetic field, it is natural to assume that the field along *z* axis (see Fig. 1) does not change the longitudinal component of the dielectric tensor, i.e., $\tilde{\epsilon}_{zz}(\mathbf{H}) = \tilde{\epsilon}_{zz}(\mathbf{H}=0)$. Within this approximation, $\tilde{\epsilon}_{zz}$ can be calculated from $\tilde{r}_p$.[14,15] The measured THz spectra of $\tilde{r}_p$ and $\tilde{\epsilon}_{zz}$ are shown in Fig. 2. Second, by using the experimental procedure described in Ref. 16 with an angle of incidence of 45°, we measure $\tilde{r}_{pp}/\tilde{r}_p$ and $\tilde{r}_{sp}/\tilde{r}_p$, which allows us to obtain $\tilde{r}_{pp}$ and $\tilde{r}_{sp}$ (see Fig. 3).

From the above complex reflection coefficients $\tilde{r}_{pp}$ and $\tilde{r}_{sp}$, we can construct the polarization plane azimuth angle ϕ and ellipticity angle η of the reflected wave (i.e., MOKE signal), as shown in Fig. 4.[16] In this system, the dielectric response in the THz frequency region originates from the intraband motion of conduction electrons. Therefore we can use the Drude model to describe the THz response. In the Drude model framework, the components of the dielectric tensor in presence of the magnetic field are the following:

$$\tilde{\epsilon}_{xx} = \epsilon_b\left[1 - \frac{\omega_p^2(\omega^2 + i\omega\Gamma)}{(\omega^2 + i\omega\Gamma)^2 - \omega^2\omega_c^2}\right],$$

$$\tilde{\epsilon}_{xy} = \frac{i\omega_p^2\epsilon_b\omega\omega_c}{(\omega^2 + i\omega\Gamma)^2 - \omega^2\omega_c^2}, \tag{7}$$

$$\tilde{\epsilon}_{zz} = \epsilon_b\left[1 - \frac{\omega_p^2}{\omega^2 + i\omega\Gamma}\right],$$

where ϵ_b is the background dielectric constant, $\omega_p = \sqrt{4\pi Ne^2/\epsilon_b m^*}$ is the plasma frequency, N and m^* are the carrier density and effective mass, Γ is the damping constant, and $\omega_c = e|\vec{H}|/m^*c$ is the cyclotron frequency. Solid lines in Fig. 4 represent this Drude model fit, which were obtained using Eqs. (2) and (4) at =1.8 THz (the corresponding carrier density is 2.1×10^{16} cm^{-3}), $\Gamma/2\pi = 0.75$ THz, $\omega_c/2\pi = 0.46$ THz, $\epsilon_b = 16.3$, and $m^* = 0.026m_e$. One can observe a pronounced resonance feature in the vicinity of plasma frequency where $\tilde{\epsilon}_{xx} \approx 0$. This effect is often referred to as the magnetoplasma resonance.[19]

By using the measured complex reflection coefficients $\tilde{r}_{pp}$ and $\tilde{r}_{sp}$, and also $\tilde{\epsilon}_{zz}$, which was obtained in the first step, we can now reconstruct the diagonal and off-diagonal component by inversely solving Eq. (2). We employed the Newton-Raphson method for this procedure.

Figure 5 shows the spectra of the obtained complex dielectric tensor. For comparison purposes we also show the

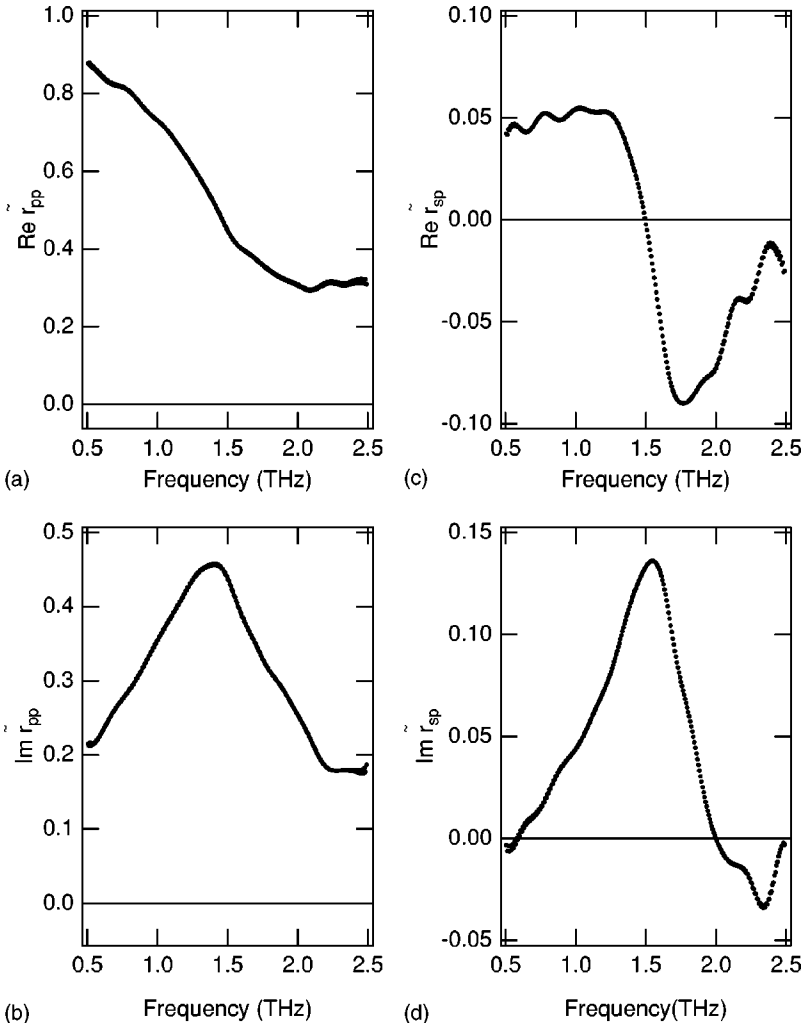

FIG. 3. Spectra of (a) $\mathrm{Re}\,\tilde{r}_{pp}$, (b) $\mathrm{Im}\,\tilde{r}_{pp}$, (c) $\mathrm{Re}\,\tilde{r}_{sp}$, and (d) $\mathrm{Im}\,\tilde{r}_{sp}$ obtained from measured $\tilde{r}_{pp}/\tilde{r}_p$, $\tilde{r}_{sp}/\tilde{r}_p$ and $\tilde{r}_p$.

complex dielectric tensor calculated with the Drude model, the parameters of which are obtained above. One can observe from Fig. 5 that $\tilde{\epsilon}_{xx}$ and $\tilde{\epsilon}_{xy}$, which are directly calculated from the complex reflection coefficients and do not rely on particular mechanism of the MOKE, correspond to the ones calculated using the Drude model with parameters obtained from the measured MOKE signal. We believe that a slightly bigger (in comparison with other components) discrepancy

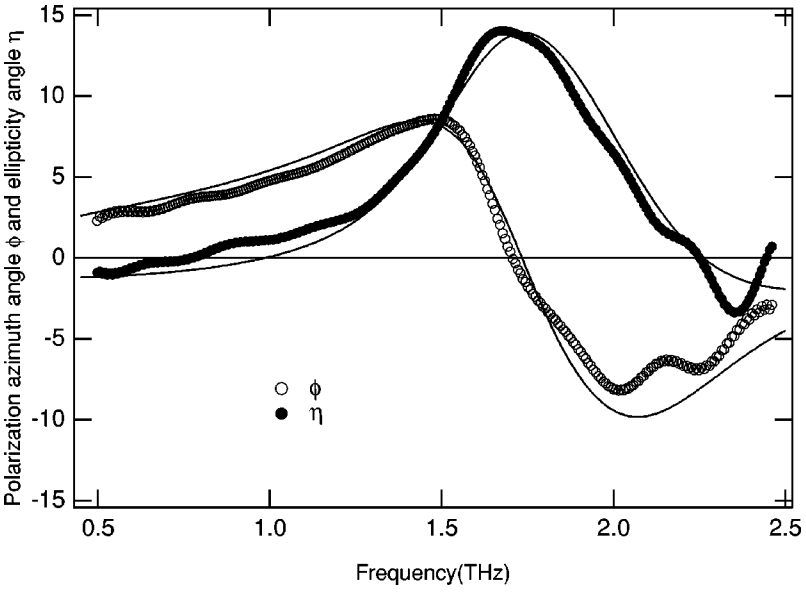

FIG. 4. The measured spectra of ϕ (circles) and η (dots) calculated from measured $\tilde{r}_{pp}/\tilde{r}_p$ and $\tilde{r}_{sp}/\tilde{r}_p$. Solid curves show the result of Drude model fitting, using Eq. (2).

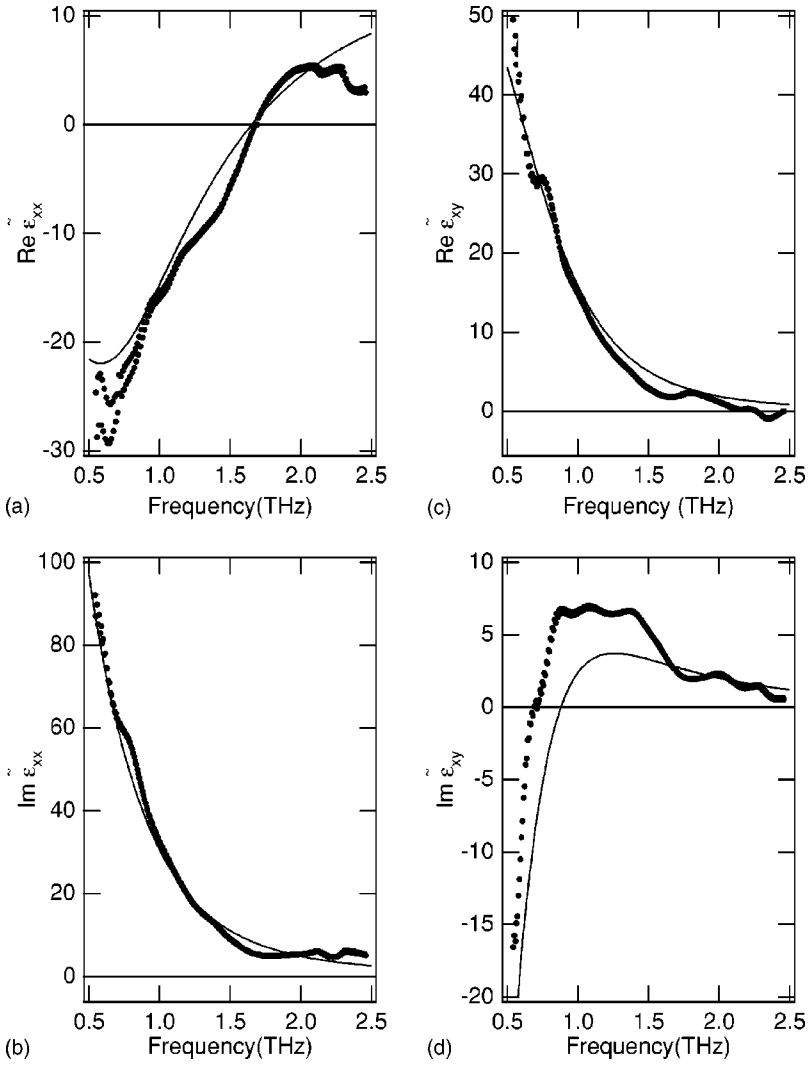

FIG. 5. Frequency dependence of (a) Re $\tilde{\epsilon}_{xx}$, (b) Im $\tilde{\epsilon}_{xx}$, (c) Re $\tilde{\epsilon}_{xy}$, and (d) Im $\tilde{\epsilon}_{xy}$ obtained from measured spectra of $\tilde{r}_{pp}$, $\tilde{r}_{sp}$, and $\tilde{r}_{p}$ (dots) and calculated spectra with Drude model with parameters obtained by fitting of MOKE signals (lines).

between the calculated Im $\tilde{\epsilon}_{xy}$ and its MOKE fit is due to the magnitude of Im $\tilde{\epsilon}_{xy}$, which is considerably smaller than the other components.

Finally we compare the conventional analysis based on SMRA with the results obtained above. Specifically, Fig. 6 shows the frequency dependence of the off-diagonal compo-

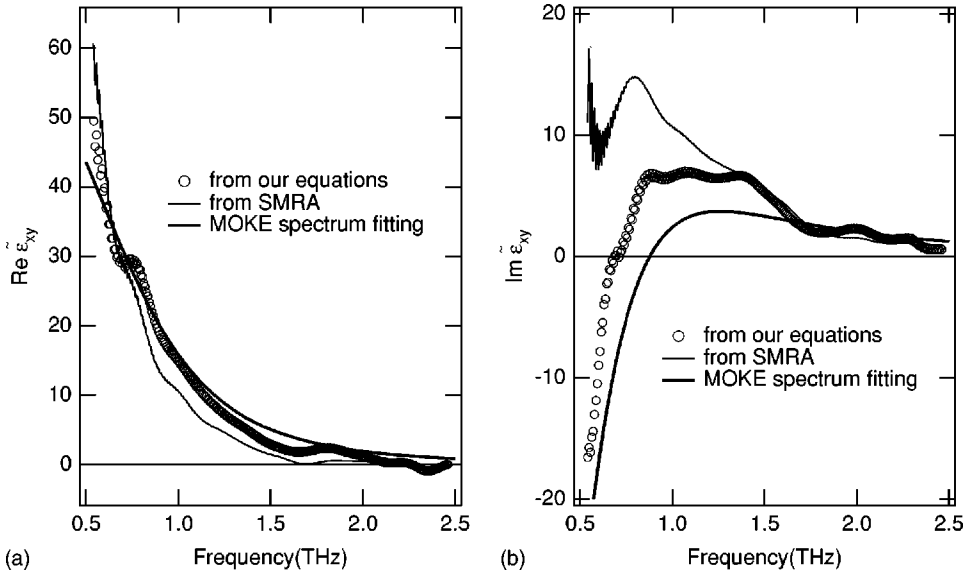

FIG. 6. Off-diagonal component of the dielectric tensor obtained from our procedure (circles), SMRA (solid line), and Drude model fitting (bold line).

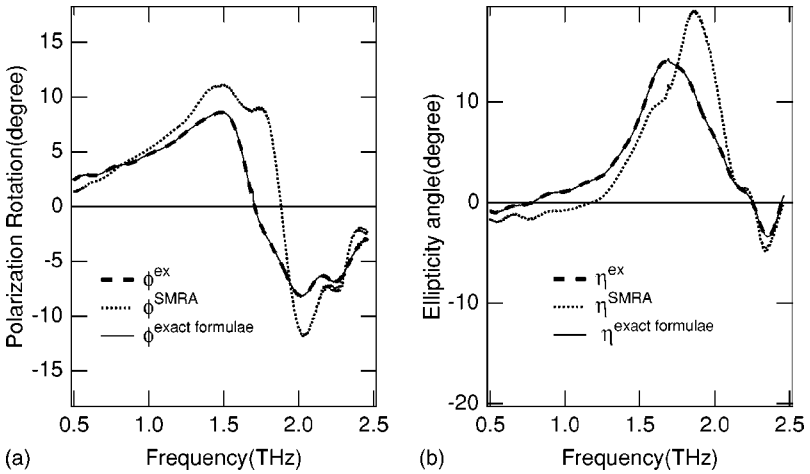

FIG. 7. Polarization azimuth (a) and ellipticity angle (b) calculated from the experimentally determined dielectric tensor using SMRA (dotted lines), calculated using exact formulas (thin solid lines), and measured in the experiment (bold broken lines).

nent of the dielectric tensor, $\tilde{\epsilon}_{xy}$, obtained from the measured $\tilde{\phi}$, and $\tilde{\epsilon}_{zz}$ by using SMRA (i.e., assuming that $|Q| \ll 1$ and $\tilde{\epsilon}_{xx} \approx \tilde{\epsilon}_{zz}$) and by using the developed method.

One can observe from Fig. 6 that the obtained off-diagonal component of the dielectric tensor, $\tilde{\epsilon}_{xy}^{ex}$, shows better correspondence with the Drude fitting of measured MOKE signals than $\tilde{\epsilon}_{xy}$, which was calculated in the SMRA framework. Results of our THz experiment[16] are apparently beyond the range of applicability of SMRA ($Q \approx 0.5$ and $|\phi + i\eta| \approx 10^{-1}$) and require a more rigorous treatment.

Figure 7 shows the spectra of the polarization rotation ϕ [Fig. 7(a)] and ellipticity angle η [Fig. 7(b)], calculated from the measured off-diagonal component of the dielectric tensor $\tilde{\epsilon}_{xy}^{ex}$ using SMRA, calculated from the exact formulas developed above, and measured in the experiment. The correspondence of the measured values and those calculated using exact expression shows the consistency of the analysis. One can observe from Fig. 7 that SMRA results in a nonnegligible departure of the polarization rotation and ellipticity angle from the measured ϕ and η in particular, in the vicinity of the plasma resonance, $\omega_p/2\pi = 1.8$ THz, when a large MOKE signal is observed.

In order to describe the difference between the developed method and SMRA, we introduce $\delta = |\tilde{\epsilon}_{xy} - \tilde{\epsilon}_{xy}^{SMRA}| / |\tilde{\epsilon}_{xy}|$, which is a quantitive measure of the SMRA imposed error. Note that here we use the dielectric tensor calculated using the Drude model with parameters obtained from the MOKE signal fits described above. From this tensor we calculate the MOKE signal $\phi + i\eta$, and calculate $\tilde{\epsilon}_{xy}^{SMRA}$ from $\phi + i\eta$ using SMRA. Figure 8(a) shows the frequency dependence of δ and $|Q| = |\tilde{\epsilon}_{xy}/\tilde{\epsilon}_{xx}|$ in the frequency range from 0.5 to 2.5 THz. In Fig. 8(b), we plot δ versus $|\phi + i\eta|$ using frequency as a parameter, where the dotted line and bold line correspond to the frequency regions above and below ω_p.

One can observe that at $\omega > \omega_p$, δ increases monotonically as $|\phi + i\eta|$ increases, indicating that the higher frequency of the incident wave from the plasma frequency, the smaller difference between the SMRA and exact analysis. At the same time, at $\omega < \omega_p$, δ is not reduced monotonically as $|\phi + i\eta|$ is reduced. From Figs. 8(a) and 8(b) one can notice that small MOKE signal does not always correspond to a small $\tilde{\epsilon}_{xy}$ (i.e., $|Q| \ll 1$). In other words, the SMRA may fail even when $|\phi + i\eta|$ is relatively small. Note that in metals, for which the magneto-optical response is conventionally studied by using the MOKE technique, $|Q|$ is the order of 10^{-2}, and SMRA is usually valid. However, a more careful analysis is necessary when the frequency of the incident wave is resonant to the intrinsic longitudinal electromagnetic modes

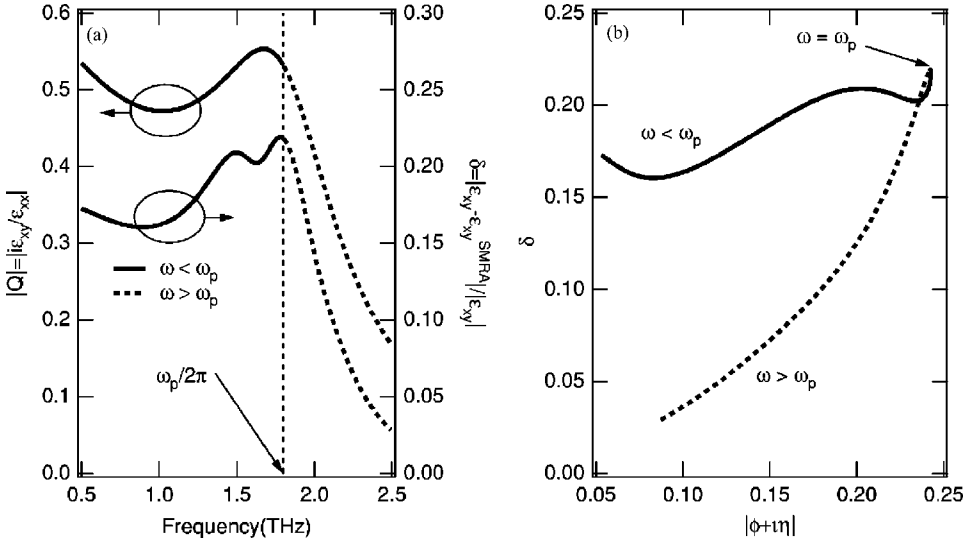

FIG. 8. SMRA versus exact analysis. (a) Frequency dependence of the magneto-optical constant Q and the error δ. (b) The relation between δ and the magnitude of MOKE signal.

of the medium, such as plasmons, optical phonons, longitudinal excitons, etc.

IV. CONCLUSION

We presented a procedure that enables us to obtain simultaneously the diagonal and off-diagonal components of the dielectric tensor by using the phase information given by time-domain THz measurements. The developed method can be applied for materials with a large magneto-optical constant $Q=i\tilde{\epsilon}_{xy}/\tilde{\epsilon}_{xx}$. By using results of the time-domain THz measurement in *n*-type undoped InAs, we demonstrate that this technique allows us to obtain both $\tilde{\epsilon}_{xx}$ and $\tilde{\epsilon}_{xy}$ directly from a MOKE experiment.

By comparing our results with those obtained from the SMRA we show that the SMRA may lead to a considerable error in the calculated components of the dielectric tensor when the probe frequency is lower than the frequency of the longitudinal electromagnetic modes even when the MOKE signal is small.

ACKNOWLEDGMENTS

This work was partially supported by Grant-in-Aid for Scientific Research (S) (Grant No. 15104006) and a Grant-in-Aid for Young Scientists(B) (Grant No. 15760002) from the Ministry of Education, Culuture, Sports, Science and Technology of Japan, and the Academy of Finland (Grant No. 200999).

APPENDIX: COMPLEX AMPLITUDE REFLECTION COEFFICIENTS FOR THE MAGNETIZED MEDIUM

In this appendix, we present the detailed description for the analysis of the plane wave reflection from an interface between isotropic medium with index refraction n_0 (medium 0) and isotropic medium under the magnetic field (medium 1). In the case of a thin film, this problem has been solved in the method based on transfer matrix formalism.[12] We cannot apply the method to media that are thicker than the penetration depth of the electromagnetic wave. In this appendix, we derive the equations which is directly applicable for an optically thick sample.

We assume that the interface coincides with plane $z=0$ and permanent magnetic field $\tilde{\mathbf{H}}$ is along the $-z$ direction, while the wave vector of the incident light wave is at angle θ_0 with the interface normal (Fig. 9). In the Cartesian coordinate system $\{xyz\}$, the dielectric tensor of the magnetized isotropic medium can be presented in the following form:

$$\tilde{\epsilon}=\begin{pmatrix}\tilde{\epsilon}_{xx} & \tilde{\epsilon}_{xy} & 0\\ -\tilde{\epsilon}_{xy} & \tilde{\epsilon}_{xx} & 0\\ 0 & 0 & \tilde{\epsilon}_{zz}\end{pmatrix}. \tag{A1}$$

In order to obtain the reflection coefficients and the polarization state of transmitted and reflected waves, it is convenient to introduce a Cartesian system $\{xy'z'\}$ with the z' axis along the wave vector of the transmitted wave (see Fig. 9). In this Cartesian coordinate system, the dielectric tensor of the magnetized medium can be presented in the following form:

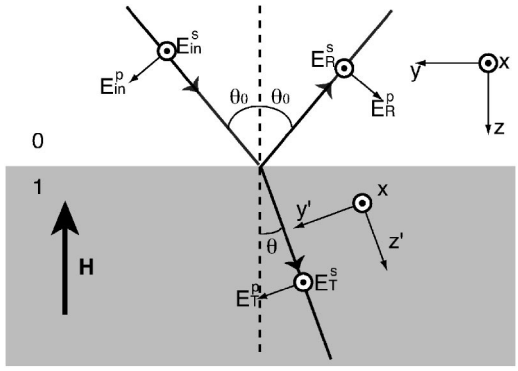

FIG. 9. The schematic configuration of the reflection problem in the plane of incidence. The definitions of the Cartesian coordinate system $\{xyz\}$ and $\{xy'z'\}$.

$$\tilde{\epsilon}=\begin{pmatrix}\tilde{\epsilon}_{xx} & \tilde{\epsilon}_{xy}\cos\tilde{\theta} & -\tilde{\epsilon}_{xy}\sin\tilde{\theta}\\ -\tilde{\epsilon}_{xy}\cos\tilde{\theta} & \tilde{\epsilon}_{xx}+\tilde{\Delta}\sin^2\tilde{\theta} & \tilde{\Delta}\sin\tilde{\theta}\cos\tilde{\theta}\\ \tilde{\epsilon}_{xy}\sin\tilde{\theta} & \tilde{\Delta}\sin\tilde{\theta}\cos\tilde{\theta} & \tilde{\epsilon}_{zz}+\tilde{\Delta}\cos^2\tilde{\theta}\end{pmatrix}, \tag{A2}$$

where $\tilde{\Delta}\equiv\tilde{\epsilon}_{zz}-\tilde{\epsilon}_{xx}$ and $\tilde{\theta}$ is the refraction angle in medium 1. The evolution equation for the amplitude of the transmitted light wave is described as follows:

$$[\tilde{n}^2(\delta_{ij}-\delta_{iz'}\delta_{jz'})-\tilde{\epsilon}_{ij}]=0, \tag{A3}$$

where $\tilde{n}$ is the refractive index and the subscripts enumerate Cartesian axes x, y', and z'. Equation (A3) has nontrivial solutions when

$$(\tilde{\epsilon}_{zz}\cos^2\tilde{\theta}+\tilde{\epsilon}_{xx}\sin^2\tilde{\theta})\tilde{n}^4-[\tilde{\epsilon}_{xx}\tilde{\epsilon}_{zz}(1+\cos^2\tilde{\theta})+(\tilde{\epsilon}^2_{xx}+\tilde{\epsilon}^2_{xy})\sin^2\tilde{\theta}]\tilde{n}^2+\tilde{\epsilon}_{zz}(\tilde{\epsilon}^2_{xx}+\tilde{\epsilon}^2_{xy})=0. \tag{A4}$$

This equation along with the Snell's law, $\tilde{n}\sin\tilde{\theta}=n_0\sin\theta_0$, allows us to arrive at two eigenvalues of the refractive index $\tilde{n}$ and the relevant refraction angle $\tilde{\theta}$. Correspondingly, the transmitted light wave can be presented in the following form:

$$\tilde{\mathbf{E}}_T=\tilde{\mathbf{E}}_A e^{-i(\omega/c)\tilde{n}_A z'}+\tilde{\mathbf{E}}_B e^{-i(\omega/c)\tilde{n}_B z'}. \tag{A5}$$

Here subscripts A and B label the modes, i.e., the solutions of Eq. (A4). The magneto-optical response of the medium results also in a nonzero longitudinal component of the transmitted light wave, i.e., $\tilde{\mathbf{E}}_{A,B}$ have nonzero projection on the propagation axis z'. Therefore we obtain the amplitudes of both p and z' components of the transmitted wave (see Fig. 9) in terms of its s component as $\tilde{E}_{pk}=\tilde{\xi}_k\tilde{E}_{sk}$ and $\tilde{E}_{zk}=\tilde{\zeta}_k\tilde{E}_{sk}$. Here subscript k labels eigenmodes A and B, while coefficients $\tilde{\xi}_k$ and $\tilde{\zeta}_k$ can be obtained from Eqs. (A2) and (A3) as the following:

$$\tilde{\xi}_k=\frac{\tilde{n}^2-\tilde{\epsilon}_{xx}-\tilde{\epsilon}^2_{xy}\sin^2\tilde{\theta}_k/\tilde{\epsilon}_{xx}+\tilde{\Delta}\cos^2\tilde{\theta}_k}{\tilde{\epsilon}_{xx}\cos\tilde{\theta}_k+\tilde{\epsilon}_{xy}\tilde{\Delta}\sin^2\tilde{\theta}_k\cos\tilde{\theta}_k/\tilde{\epsilon}_{xx}+\tilde{\Delta}\cos^2\tilde{\theta}_k}, \tag{A6}$$

$$\tilde{\zeta}_k = -\frac{\tilde{\epsilon}_{xy}^2 + \tilde{\Delta}(\tilde{n}_k^2 - \tilde{\epsilon}_{xx})}{\tilde{\epsilon}_{zz}\tilde{\epsilon}_{xy}} \sin\tilde{\theta}_k. \tag{A7}$$

We will restrict ourselves to the polarization effects with the *p*-polarized incident light wave; however, the magneto-optical response ensures the existence of the both *s*- and *p*-polarized components in the reflected and transmitted waves (see Fig. 9). In the Cartesian frame $\{xyz\}$, in which the vacuum-medium interface coincides with the plane $z=0$, the electric ($\tilde{\mathbf{E}}$) and magnetic ($\tilde{\mathbf{H}}$) fields of the incident (labeled by subscript *I*) and reflected (*R*) waves can be presented in the following form:

$$\tilde{\mathbf{E}}_I = (0, \tilde{E}_{Ip}\cos\theta_0, \tilde{E}_{Ip}\sin\theta_0),$$

$$\tilde{\mathbf{H}}_I = (-\tilde{E}_{Ip}, 0, 0)\frac{n_0}{c}, \tag{A8}$$

$$\tilde{\mathbf{E}}_R = (\tilde{E}_{Rs}, -\tilde{E}_{Rp}\cos\theta_0, \tilde{E}_{Rp}\sin\theta_0),$$

$$\tilde{\mathbf{H}}_R = (-\tilde{E}_{Rp}, -\tilde{E}_{Rs}\cos\theta_0, \tilde{E}_{Rs}\sin\theta_0)\frac{n_0}{c}. \tag{A9}$$

As we have shown in Eq. (A5), the transmitted wave consists of two eigenmodes; the complex amplitude in the Cartesian $\{xyz\}$ frame and relevant magnetic fields are the following:

$$\tilde{\mathbf{E}}_k = (\tilde{E}_{sk}, \tilde{E}_{pk}\cos\tilde{\theta}_k - \tilde{E}_{zk}\sin\tilde{\theta}_k, \tilde{E}_{pk}\sin\tilde{\theta}_k + \tilde{E}_{zk}\cos\tilde{\theta}_k),$$

$$\tilde{\mathbf{H}}_k = (-\tilde{E}_{pk}, \tilde{E}_{sk}\cos\tilde{\theta}_k, -\tilde{E}_{sk}\sin\tilde{\theta}_k)\frac{\tilde{n}_k}{c}, \tag{A10}$$

where $k=A,B$. The continuity of the tangential components of the electric and magnetic field at $z=0$ implies

$$\tilde{E}_{Rs} = \tilde{E}_{sA} + \tilde{E}_{sB},$$

$$\tilde{E}_{Ip}\cos\theta_0 - \tilde{E}_{Rp}\cos\theta_0 = \tilde{\chi}_A\tilde{E}_{sA} + \tilde{\chi}_B\tilde{E}_{sB},$$

$$-n_0\tilde{E}_{Ip} - n_0\tilde{E}_{Rp} = -\tilde{n}_A\tilde{\xi}_A\tilde{E}_{sA} - \tilde{n}_B\tilde{\xi}_B\tilde{E}_{sB},$$

$$-n_0\tilde{E}_{Rs}\cos\theta_0 = \tilde{n}_A\tilde{E}_{sA}\cos\tilde{\theta}_A + \tilde{n}_B\tilde{E}_{sB}\cos\tilde{\theta}_B, \tag{A11}$$

where

$$\tilde{\chi}_k = \tilde{\xi}_k\cos\tilde{\theta}_k - \tilde{\zeta}_k\sin\tilde{\theta}_k. \tag{A12}$$

Solution of the set of Eqs. (A11) gives the following expressions for the amplitude reflection coefficients:

$$\tilde{r}_{pp} = \frac{\tilde{E}_{Rp}}{\tilde{E}_{Ip}} = \frac{(\tilde{n}_A\tilde{\xi}_A - n_0\tilde{\chi}_A/\cos\theta_0)\tau_B - (\tilde{n}_B\tilde{\xi}_B - n_0\tilde{\chi}_B/\cos\theta_0)\tau_A}{(\tilde{n}_A\tilde{\xi}_A + n_0\tilde{\chi}_A/\cos\theta_0)\tau_B - (\tilde{n}_B\tilde{\xi}_B + n_0\tilde{\chi}_B/\cos\theta_0)\tau_A}, \tag{A13}$$

$$\tilde{r}_{sp} = \frac{\tilde{E}_{Rs}}{\tilde{E}_{Ip}} = \frac{2n_0(\tilde{n}_B\cos\tilde{\theta}_B - \tilde{n}_A\cos\tilde{\theta}_A)}{(\tilde{n}_A\tilde{\xi}_A + n_0\tilde{\chi}_A/\cos\theta_0)\tau_B - (\tilde{n}_B\tilde{\xi}_B + n_0\tilde{\chi}_B/\cos\theta_0)\tau_A}, \tag{A14}$$

where

$$\tau_k = \tilde{n}_k\cos\tilde{\theta}_k + n_0\cos\theta_0. \tag{A15}$$

It should be noted here that Eqs.(A13) and (A14) are valid for an oblique incidence and any magnitude of the magneto-optical response.

In the following we compare these equations with the SMRA. The difference between mode *A* and *B* is reduced to the difference of the sign of magneto-optical response; therefore we use + and − for subscripts instead of *A* and *B*. Substituting the SMRA condition, i.e., $|Q| = |i\tilde{\epsilon}_{xy}|/|\tilde{\epsilon}_{xx}| \ll 1$ and $\tilde{\Delta}\approx 0$ in Eq. (A4), one obtains

$$\tilde{n}_k = \tilde{n}\left(1 \pm \frac{i\tilde{\alpha}\tilde{Q}}{2}\right),$$

$$\sin\tilde{\theta}_k = \frac{n_0\sin\theta_0}{\tilde{n}}\left(1 \mp \frac{i\tilde{\alpha}\tilde{Q}}{2}\right), \tag{A16}$$

where $\tilde{\alpha} = \sqrt{n_0^2\sin^2\theta_0/\tilde{\epsilon}_{zz} - 1}$. $\tilde{n} = \sqrt{\tilde{\epsilon}_{zz}}$ is the index of refraction of the medium 1 without magnetic field. With these values we can reduce the quantities $\tilde{\xi}_k$, $\tilde{\zeta}_k$, and $\tilde{\chi}_k$ as follows:

$$\tilde{\xi}_k = \frac{\mp\tilde{\alpha} - i\tilde{Q}\sin^2\tilde{\theta} + i(\tilde{\alpha}^2\tilde{Q}/2)\tan^2\tilde{\theta}}{\cos\tilde{\theta}},$$

$$\tilde{\zeta}_k = i\tilde{Q}\sin\tilde{\theta},$$

$$\tilde{\chi}_k = \mp\tilde{\alpha} - 2i\tilde{Q}\sin^2\tilde{\theta}.$$

Substituting these values into Eqs. (A13) and (A14), one obtains

$$\tilde{r}_{pp} = \frac{\tilde{n}\cos\theta_0 - n_0\cos\tilde{\theta}}{\tilde{n}\cos\theta_0 + n_0\cos\tilde{\theta}},$$

$$\tilde{r}_{sp} = \frac{i\tilde{Q}n_0\tilde{n}\cos\theta_0}{(\tilde{n}\cos\tilde{\theta} + n_0\cos\theta_0)(\tilde{n}\cos\theta_0 + n_0\cos\tilde{\theta})\cos\tilde{\theta}}. \tag{17}$$

These are completely the same as Eq. (2.31) of Ref. 9. By these quantities on obtain the MOKE signal as Eq. (5).

*Present address: Department of Physics, the University of Tokyo, Hongo, Bunkyo-ku, Tokyo, 113-0033, Japan.

†Author to whom correspondence should be addressed. Email address: gonokami@ap.t.u-tokyo.ac.jp

[1] S. A. Wolf, D. D. Awschalom, R. A. Buhrman, J. M. Daughton, S. von Molnár, M. L. Roukes, A. Y. Chtchelkanova, and D. M. Treger, Science **294**, 1488 (2001).

[2] Z. Q. Qiu and S. D. Bader, J. Magn. Magn. Mater. **200**, 664 (1999).

[3] E. Beaurepaire, J.-C. Merle, A. Daunois, and J.-Y. Bigot, Phys. Rev. Lett. **76**, 4250 (1996).

[4] T. Kise, T. Ogasawara, M. Ashida, Y. Tomioka, Y. Tokura, and M. Kuwata-Gonokami, Phys. Rev. Lett. **85**, 1986 (2000).

[5] P. N. Argyres, Phys. Rev. **97**, 334 (1955).

[6] H. S. Benett and E. A. Stern, Phys. Rev. **137**, A448 (1965).

[7] P. S. Pershan, J. Appl. Phys. **38**, 1482 (1967).

[8] J. F. Dillon, *Magneto-optical Properties of Magnetic Crystals*, Vol. 13 of *Inter-University Electronics Series* (McGraw-Hill, New York, 1988), Chap. 5, p. 149.

[9] P. M. Oppeneer, *Magneto-optical Kerr Spectra*, Vol. 13 of *Handbook of Magnetic Materials* (Elsevier Science, Amsterdam; Tokyo, 2001), Chap. 3, p. 229.

[10] A. Berger and M. R. Pufall, Appl. Phys. Lett. **71**, 965 (1997).

[11] M. Schubert, B. Rheinländer, J. A. Woollam, B. Johs, and C. M. Herzinger, J. Opt. Soc. Am. A **13**, 875 (1996).

[12] M. Schubert, T. E. Tiwald, and J. A. Woolam, Appl. Opt. **38**, 177 (1999).

[13] M. Schubert and T. Hofmann, J. Opt. Soc. Am. A **20**, 347 (2003).

[14] M. C. Nuss, J. Orenstein, and G. Grüner, *Terahertz Time-Domain Spectroscopy*, Vol. 74 of *Topics in Applied Physics* (Springer, Berlin Heidelberg, 1998), Chap. 3, p. 7.

[15] T.-I. Jeon and D. Grischkowsky, Appl. Phys. Lett. **72**, 3032 (1998).

[16] R. Shimano, Y. Ino, Y. P. Svirko, and M. Kuwata-Gonokami, Appl. Phys. Lett. **81**, 199 (2002).

[17] M. Born and E. Wolf, *Principles of Optics*, 6th ed. (Pergamon, Oxford; Tokyo, 1980), Chap. 1.

[18] K. Sato, Jpn. J. Appl. Phys. **20**, 2403 (1981).

[19] B. Lax and G. B. Wright, Phys. Rev. Lett. **4**, 16 (1960).